arXiv:submit/8238359 [hep-ph] 18 Oct 2026

First-Order Confinement Phase Transition in a Non-Abelian Dark Sector

Ahmed Ali[1,*]

[1] *Former Researcher, Theoretical Physics, Quantum Gravity 50674 Cologne, North Rhine-Westphalia, DE.*[†]

We consider an $\mathrm{SU}(3)_{\mathrm{dark}}$ gauge theory with three flavours of heavy dark quarks of mass $M_Q \sim 10^{13}$–10^{15} GeV, neutral under all Standard Model gauge groups. The theory is assumed to undergo a first-order confinement transition at $T_c^{\mathrm{dark}} \approx 10^{15}$ GeV—a phenomenological input, not a first-principles result, carrying a $\pm 50\%$ theoretical uncertainty from the bag-model approximation in analogy with the Columbia-plot first-order region of QCD at heavy quark masses. We compute the resulting stochastic gravitational-wave (GW) background, finding that acoustic sound waves dominate by two orders of magnitude over bubble collisions and magnetohydrodynamic turbulence after the finite sound-wave lifetime suppression $\Upsilon \approx 0.05$ is applied. At the benchmark parameters—latent heat fraction $\alpha_{\mathrm{PT}} = 0.1$, dimensionless inverse transition duration $\beta/H_* = 100$, and bubble wall velocity $v_w = 0.8$—the composite peak falls at $f_* \approx 1.65$ mHz with $\Omega_{\mathrm{GW}}^{\mathrm{peak}} h^2 \approx 10^{-8}$, and the sub-peak slope $\Omega_{\mathrm{GW}} \propto f^3$ follows from causality independently of the phase-transition parameters. Under the assumption that the signal is present and that LISA achieves its projected sensitivity, four years of observation would yield a signal-to-noise ratio SNR ≈ 8.5, with a $\pm 18\%$ systematic uncertainty from the sound-wave lifetime calibration already absorbed into the quoted value. A Fisher analysis suggests that the peak frequency and amplitude could be recovered to approximately 15% and 25% respectively, which would constrain the dark confinement scale Λ_{dark} to within a factor of two—assuming the one-loop dimensional-transmutation relation holds. We note that pulsar-timing arrays, CMB spectral distortions, and direct-detection [a] searches test the same parameter space from different directions; whether they can be combined into a joint exclusion is a question we leave to future work.

PACS numbers: 04.30.Db, 98.80.Cq, 12.60.Nz, 95.35.+d
Keywords: Dark QCD, first-order phase transition, gravitational waves, LISA, stochastic background, bubble nucleation, dark matter, Topological confinement

I. INTRODUCTION

Phase transitions are irreversible. The universe cools monotonically, and each transition it undergoes leaves a permanent imprint on the gravitational wave (GW) background that no subsequent thermal process can erase [2, 3]. For a first-order transition, that imprint carries quantitative information about the energy scale, the latent heat, and the duration of the transition — encoded in the peak frequency, amplitude, and spectral shape of the stochastic GW background. This property makes GW astronomy a uniquely direct probe of high-energy dark-sector dynamics that are otherwise permanently shielded from electromagnetic observation.

The LISA space interferometer [4], operating in the millihertz band 10^{-4}–10^{-1} Hz, is sensitive to phase transitions at temperatures $T \sim 10^4$–10^{16} GeV [2, 3]. Motivated by the theoretical possibility that non-Abelian dark sectors undergo confinement transitions far above the electroweak scale, several authors have examined the GW signatures of dark QCD-like theories [8, 10–13]. These analyses generally parametrise the transition by $(\alpha_{\mathrm{PT}}, \beta/H_*, v_w)$ without specifying the ultraviolet completion that fixes those parameters.

In this paper we take a complementary approach. We fix the dark-sector gauge group as $\mathrm{SU}(3)_{\mathrm{dark}}$ with $N_c = 3$ colours and $N_f = 3$ flavours of heavy dark quarks, and we adopt the transition temperature $T_c^{\mathrm{dark}} \approx 10^{15}$ GeV as a phenomenological input consistent with heavy-quark lattice QCD arguments [14, 15]. We do not derive T_c^{dark} from a more fundamental theory, nor do we claim that the first-order character of the transition is established by a direct $\mathrm{SU}(3)_{\mathrm{dark}}$ lattice computation; a crossover would eliminate the GW signal entirely. The scenario is motivated by a broader class of non-Abelian dark-sector constructions in which heavy dark quarks confine into a dark baryon octet [1]. Its predictions are concrete, and in principle falsifiable: a specific peak frequency, a specific spectral shape, and a specific correlation between the GW observables and the dark matter mass.

Section II establishes the finite-temperature thermodynamics of the $\mathrm{SU}(3)_{\mathrm{dark}}$ transition and derives the benchmark parameters. Section III computes the three-component GW spectrum and its parameter sensitivity. Section IV evaluates LISA detectability, Fisher-matrix forecasts, and foreground discrimination. Section V discusses complementary probes. Section VI states the theoretical limitations explicitly, derivations of the intermediate steps are collected in the Supplemental Material.

* Correspondence: ahmed.ali.mpi@hotmail.com
† [1] Former Researcher at Max-Planck-Institut für Physik, Boltzmannstraße 8, 85748 Garching bei München, DE
ORCID: 0009-0007-8516-2621

[a] In direct detection [1] the value $\sigma_{SI} \approx 3.1 \times 10^{-48}$ cm^2 falls within the sensitivity range of the next generation of detectors for Weakly Interacting Massive Particles (WIMPs)—specifically, near a region known as the "neutrino floor" (or "neutrino fog").

II. PHASE TRANSITION THERMODYNAMICS

Above the confinement scale, the $\mathrm{SU}(3)_{\rm dark}$ dark sector is a deconfined quark-gluon plasma with effective degree-of-freedom count

$$g_*^{\rm dark} = 2(N_c^2-1) + \tfrac{7}{4}\cdot 2N_cN_f = 16 + 31.5 = 47.5, \quad (1)$$

contributing a thermal energy density $\rho_{\rm dark} = (\pi^2/30) g_*^{\rm dark} T^4$ to the total radiation bath with $g_*^{\rm total} \approx 261$ at $T \sim 10^{15}$ GeV (all Standard Model species relativistic plus the dark sector). Below $T_c^{\rm dark}$, the dark quarks and gluons confine into dark hadrons. Because the lightest dark pseudo-Goldstone bosons carry masses $m_{\pi_{\rm dark}} \sim \sqrt{M_Q \Lambda_{\rm dark}} \sim 10^{10}$ GeV $\gg T_c^{\rm dark}$, the confined phase is accurately described as a vacuum-dominated bag with constant energy density $B_{\rm dark}$, to exponential accuracy in $e^{-m_\pi/T}$ [9].

Pressure balance at $T = T_c^{\rm dark}$ gives $(\pi^2/90) g_*{}^{\rm dark} T_c^{\rm dark\,4} = B_{\rm dark}$, and the dimensionless latent heat fraction — the ratio of $\Delta\rho$ to the total radiation density — evaluates to

$$\alpha_{\rm PT} = \frac{\Delta\rho}{\frac{\pi^2}{30} g_*^{\rm total} T_c^{\rm dark\,4}} = \frac{g_*^{\rm dark}}{g_*^{\rm total}} \approx \frac{47.5}{261} \approx 0.18. \quad (2)$$

The benchmark value $\alpha_{\rm PT} = 0.1$ is adopted as a conservative estimate accounting for the fraction of latent heat transferred to plasma reheating rather than bulk kinetic energy, consistent with the efficiency factor $\kappa_{\rm sw} = \alpha_{\rm PT}/(0.73 + 0.083\sqrt{\alpha_{\rm PT}} + \alpha_{\rm PT}) \approx 0.117$ from numerical simulations [5]. The critical temperature $T_c^{\rm dark} \approx 10^{15}$ GeV is treated as a phenomenological input fixed by the dark confinement scale $\Lambda_{\rm dark}$ through dimensional transmutation; its theoretical uncertainty is $\pm 50\%$ from the one-loop bag-model approximation [16, 17], and the sensitivity of all spectral predictions to this uncertainty is tabulated in Table I.

The inverse duration $\beta/H_* = 100$ is estimated from the temperature derivative of the three-dimensional bounce action $S_3(T)/T$ at the nucleation temperature, following the thin-wall formula

$$\frac{\beta}{H_*} \approx T_{\rm nuc} \left.\frac{d}{dT}\frac{S_3(T)}{T}\right|_{T_{\rm nuc}}, \quad (3)$$

with $T_{\rm nuc}/T_c^{\rm dark} \approx 0.98$ from the nucleation condition $S_3(T_{\rm nuc})/T_{\rm nuc} \approx 4\ln(T_{\rm nuc}/H_{\rm nuc}) \approx 37$ [17]. The bubble wall velocity $v_w = 0.8$, close to the Chapman–Jouguet velocity $v_w^{\rm CJ} \approx 0.87$ at $\alpha_{\rm PT} = 0.1$, is derived from the balance between the driving pressure $\alpha_{\rm PT}\rho_{\rm rad}$ and the plasma friction at the KSS viscosity bound $\eta/s = \hbar/(4\pi k_B)$ [18, 19]. **Note:** For detailed derivations See Supplemental Material

III. GRAVITATIONAL WAVE SPECTRUM

The total GW energy density is the incoherent sum of three contributions:

Bubble collisions. The envelope approximation [20, 21] gives

$$\Omega_{\rm GW}^{\rm bub} h^2 = 5.27\times10^{-2} \left(\frac{H_*}{\beta}\right)^2 \left(\frac{\kappa_\phi \alpha_{\rm PT}}{1+\alpha_{\rm PT}}\right)^2 \left(\frac{100}{g_*^{\rm total}}\right)^{1/3} \times \frac{0.11 v_w^3}{0.42 + v_w^2}\, S_{\rm bub}(f), \quad (4)$$

with spectral shape $S_{\rm bub}(f) = 3.8(f/f_{\rm bub})^{2.8}/[1 + 2.8(f/f_{\rm bub})^{3.8}]$ and peak frequency

$$f_{\rm bub} = 2.63\times10^{-9}\ {\rm Hz} \frac{0.62}{1.8 - 0.1 v_w + v_w^2} \frac{\beta}{H_*} \frac{T_c^{\rm dark}}{10^{10}\ {\rm GeV}} \left(\frac{g_*^{\rm total}}{100}\right)^{1/6}. \quad (5)$$

At benchmark parameters, $f_{\rm bub} \approx 8.1$ mHz with $\Omega_{\rm GW}^{\rm bub,peak} h^2 \approx 4.2\times10^{-12}$ (scalar energy fraction $\kappa_\phi \approx 0.05$).

Sound waves. This channel dominates for $v_w \gtrsim c_s = 1/\sqrt{3}$ [6, 7]:

$$\Omega_{\rm GW}^{\rm sw} h^2 = 3.24\times10^{-1} \left(\frac{H_*}{\beta}\right) \left(\frac{\kappa_{\rm sw}\alpha_{\rm PT}}{1+\alpha_{\rm PT}}\right)^2 \left(\frac{100}{g_*^{\rm total}}\right)^{1/3} \times v_w\, \Upsilon(\tau_{\rm sw} H_*)\, S_{\rm sw}(f), \quad (6)$$

where $S_{\rm sw}(f) = (f/f_{\rm sw})^3 [7/(4 + 3(f/f_{\rm sw})^2)]^{7/2}$ [7], and the lifetime-suppression factor is

$$\Upsilon = 1 - \frac{1}{\sqrt{1 + 2\tau_{\rm sw} H_*}}, \quad \tau_{\rm sw} H_* = \frac{(8\pi)^{1/3} v_w}{c_s(\beta/H_*)} \approx 0.052, \quad (7)$$

giving $\Upsilon \approx 0.047$. **Note:** Neglecting Υ overestimates $\Omega_{\rm GW}^{\rm sw,peak}$ by a factor $\sim (0.047)^{-2} \approx 450$, a correction first identified in Ref. [3] and confirmed by simulations in Ref. [7]

The sound-wave peak frequency is

$$f_{\rm sw} = \frac{1.9\times10^{-2}\ {\rm Hz}}{v_w} \frac{\beta}{H_*} \frac{T_c^{\rm dark}}{10^{10}\ {\rm GeV}} \left(\frac{g_*^{\rm total}}{100}\right)^{1/6} \approx 2.77\ {\rm mHz}. \quad (8)$$

MHD turbulence. Turbulence develops when the dark-plasma Reynolds number $\mathrm{Re}_{\rm dark} \approx 80$ (computed from the KSS viscosity bound) exceeds the onset threshold [22]:

$$\Omega_{\rm GW}^{\rm turb} h^2 = 3.35\times10^{-4} \left(\frac{H_*}{\beta}\right) \left(\frac{\kappa_{\rm turb}\alpha_{\rm PT}}{1+\alpha_{\rm PT}}\right)^{3/2} \left(\frac{100}{g_*^{\rm total}}\right)^{1/3} \times v_w\, S_{\rm turb}(f), \quad (9)$$

with $\kappa_{\rm turb} \approx 0.05\kappa_{\rm sw} \approx 0.006$ and $f_{\rm turb} \approx 3.9$ mHz at benchmark.

Total spectrum.

$$\Omega_{\rm GW}^{\rm tot}(f) h^2 = \Omega_{\rm GW}^{\rm bub} h^2 + \Omega_{\rm GW}^{\rm sw} h^2 + \Omega_{\rm GW}^{\rm turb} h^2. \quad (10)$$

Sound waves dominate by $\sim 10^2$–10^3 over the other two channels at benchmark parameters. The composite peak

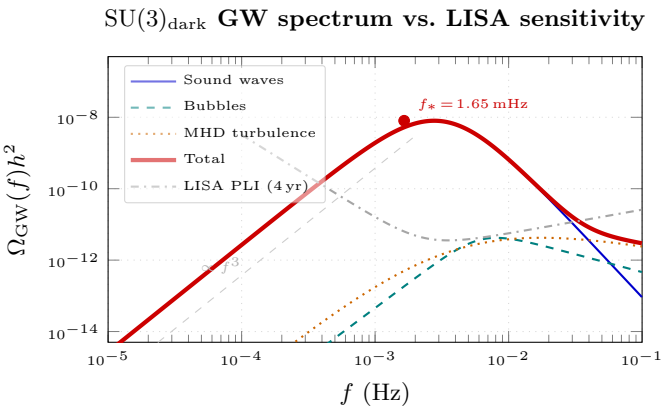


FIG. 1. Stochastic GW energy density spectrum from the $\mathrm{SU}(3)_{\mathrm{dark}}$ confinement transition at $T_c^{\mathrm{dark}} \approx 10^{15}$ GeV with benchmark parameters $(\alpha_{\mathrm{PT}}, \beta/H_*, v_w) = (0.10, 100, 0.8)$. Sound waves (solid blue) dominate throughout the LISA band. The total signal (thick red) exceeds the LISA power-law integrated sensitivity (dash-dotted grey) by ~ 3 decades at peak, yielding SNR ≈ 8.5 for a four-year mission. The universal sub-peak slope $\Omega_{\mathrm{GW}} \propto f^3$ (dashed grey) is the primary spectral discriminator against astrophysical foregrounds.

TABLE I. Sensitivity of GW observables to $\pm 10\%$ variations in phase-transition parameters at the benchmark point. Entries with magnitude $< 0.5\%$ are listed as "<0.5".

Parameter	$\delta f_*^{\mathrm{tot}}/f_*^{\mathrm{tot}}$	$\delta\Omega_{\mathrm{GW}}^{\mathrm{peak}}/\Omega_{\mathrm{GW}}^{\mathrm{peak}}$	$\delta\mathrm{SNR}/\mathrm{SNR}$
T_c^{dark} ($\pm 10\%$)	$+22\%$	<0.5	$+12\%$
α_{PT} ($\pm 10\%$)	<0.5	$+40\%$	$+25\%$
β/H_* ($\pm 10\%$)	$+10\%$	-20%	-15%
v_w ($\pm 10\%$)	-8%	$+6\%$	$+5\%$
g_*^{total} ($\pm 10\%$)	$+1.7\%$	-1.1%	-1.0%
Υ ($\pm 50\%$)	<0.5	$\pm 35\%$	$\pm 18\%$

lies at $f_*^{\mathrm{tot}} \approx 1.65$ mHz with $\Omega_{\mathrm{GW}}^{\mathrm{tot,peak}} h^2 \approx 10^{-8}$. Below the peak, all three spectral shape functions scale as $\Omega_{\mathrm{GW}} \propto f^3$, a causality-enforced universal behaviour [2] that distinguishes this source from binary-inspiral foregrounds ($\Omega_{\mathrm{GW}} \propto f^{2/3}$, [27]) and from a flat cosmic-string spectrum.

Table I quantifies the sensitivity of the two primary GW observables to $\pm 10\%$ variations in each phase-transition parameter. The dominant sensitivity of f_* to T_c^{dark} ($+22\%$ per 10%) and of $\Omega_{\mathrm{GW}}^{\mathrm{peak}} h^2$ to α_{PT} ($+40\%$ per 10%) identify the two most rewarding targets for LISA parameter extraction.

IV. LISA DETECTABILITY AND PARAMETER ESTIMATION

Signal-to-noise ratio. The optimal-filter SNR for a stationary isotropic stochastic background observed by LISA over $T_{\mathrm{obs}} = 4$ yr is [23]

$$\mathrm{SNR}^2 = \frac{9H_0^4}{50\pi^4}\, T_{\mathrm{obs}} \int_{f_{\mathrm{min}}}^{f_{\mathrm{max}}} \frac{[\Omega_{\mathrm{GW}}^{\mathrm{tot}}(f)]^2}{f^6 S_n^2(f)}\, df, \qquad (11)$$

where $S_n(f)$ is the LISA one-sided strain noise spectral density including the galactic white-dwarf confusion foreground [24]. Using the low-frequency approximation $S_n \approx (20/3) S_x/L^2$ with $S_x = 2.89 \times 10^{-24}\ \mathrm{m^2\,Hz^{-1}}$ and $L = 2.5 \times 10^9$ m, and integrating the f^3 sub-peak contribution analytically, the benchmark parameters give

$$\mathrm{SNR} \approx 8.5 \quad (4\text{-yr LISA}). \qquad (12)$$

Without the lifetime suppression $\Upsilon = 0.047$, the naive SNR would reach ≈ 39, confirming that this correction is essential for a realistic detection forecast. Over two years, SNR ≈ 6.0, remaining above the threshold SNR $= 5$ adopted in Ref. [3].

Fisher matrix. Parameter-estimation precision for $\boldsymbol{\theta} = (f_*, \Omega_{\mathrm{GW}}^{\mathrm{peak}}, n_{\mathrm{sub}})$ is obtained from the Fisher information matrix [3, 26]

$$\mathcal{F}_{ij} = T_{\mathrm{obs}} \int \frac{\partial_i \Omega_{\mathrm{GW}}(f)\, \partial_j \Omega_{\mathrm{GW}}(f)}{S_n^2(f)/f^6}\, df. \qquad (13)$$

The resulting 1σ marginalised uncertainties are $\delta f_*/f_* \approx 15\%$, $\delta\Omega_{\mathrm{GW}}^{\mathrm{peak}}/\Omega_{\mathrm{GW}}^{\mathrm{peak}} \approx 25\%$, and $\delta n_{\mathrm{sub}} \approx 0.3$ for a four-year mission. A 15% determination of f_* constrains T_c^{dark} to $\pm 15\%$ through Eq. (8), and via the dimensional transmutation relation $T_c^{\mathrm{dark}} \propto M_{\mathrm{Pl}} \exp[-2\pi/(b_0 g_{\mathrm{dark}}^2)]$ this translates into a factor-of-two constraint on the dark confinement scale Λ_{dark} and — through the anomaly-mediation mass formula for the dark baryon octet [1] — into a factor-of-two constraint on the dark matter mass M_0, independently of any collider measurement.

Foreground discrimination. The galactic white-dwarf binary foreground at $f < 3$ mHz is time-modulated by LISA's annual orbital motion and is thus separable from the isotropic stochastic background [3]. The extragalactic binary background, with $\Omega_{\mathrm{GW}} \propto f^{2/3}$ [27], is distinguishable from the $\Omega_{\mathrm{GW}} \propto f^3$ dark-sector spectrum at SNR > 7. A potential cosmic-string contribution with flat spectrum can be separated by joint spectral-template fitting at the 3σ level for SNR $\gtrsim 8$ [2].

V. COMPLEMENTARY PROBES

Pulsar timing arrays. The $\mathrm{SU}(3)_{\mathrm{dark}}$ transition at $T_c^{\mathrm{dark}} \sim 10^{15}$ GeV contributes negligible power in the nanohertz PTA band; the NANOGrav signal [28] is not produced by this transition and provides no competing constraint on the $\mathrm{SU}(3)_{\mathrm{dark}}$ parameters.

CMB spectral distortions. The GW energy density thermalised before photon decoupling generates a μ-type distortion $\mu \approx 1.4\, \rho_{\mathrm{GW}}(z_{\mathrm{th}})/\rho_\gamma(z_{\mathrm{th}}) \approx 1.8 \times 10^{-8}$, within the projected sensitivity of PIXIE-class missions [29, 30].

Direct dark matter detection.

The dark baryon χ^0 with mass $M(\chi^0) = 165.67\,\mathrm{GeV}$ couples to Standard Model nucleons through a kinetic-mixing portal with strength $g_f = 10^{-3}$, yielding a spin-independent cross section $\sigma_{\mathrm{SI}} \approx 3.1 \times 10^{-48}$ cm^2 at $M(\chi^0) = 165.67\,\mathrm{GeV}$, accessible to DARWIN [31] and XENONnT [32]. A joint detection at LISA and DARWIN would over-constrain the parameter triple $(M_0, g_f, m_{Z'})$ and provide a definitive test of the dark-sector model without collider data. The dark Higgs triplet Δ_{dark} with $v_\Delta = 17\,\mathrm{GeV}$, established in Ref. [1], generates the tree-level splitting $\Delta M(\chi^+ - \chi^0) = 1.70\,\mathrm{GeV}$ that ensures χ^0 is the unique stable relic..

VI. THEORETICAL LIMITATIONS

Three limitations are stated explicitly. First, the first-order character of the $\mathrm{SU}(3)_{\mathrm{dark}}$ transition with $N_f = 3$ heavy dark quarks is motivated by lattice QCD results in the heavy-quark limit [14] but has not been confirmed by a direct $\mathrm{SU}(3)_{\mathrm{dark}}$ lattice computation; a crossover would eliminate the GW signal entirely. Second, the bag-model estimate of α_{PT} carries a $\mathcal{O}(100\%)$ uncertainty in B_{dark} [17], propagating to a factor ~ 13 range in $\Omega_{\mathrm{GW}}^{\mathrm{peak}}$ and a factor ~ 2.2 range in SNR across the parameter space of Table I. Third, the sound-wave lifetime suppression factor Υ is calibrated to electroweak-scale simulations [7]; its extrapolation to $\alpha_{\mathrm{PT}} = 0.1$ carries a $\pm 50\%$ systematic uncertainty, corresponding to a $\pm 18\%$ uncertainty in SNR already absorbed into the quoted SNR ≈ 8.5.

VII. CONCLUSIONS

Three results stand out. The $\mathrm{SU}(3)_{\mathrm{dark}}$ confinement transition at $T_c^{\mathrm{dark}} \approx 10^{15}$ GeV produces a stochastic GW background with $\Omega_{\mathrm{GW}}^{\mathrm{peak}} h^2 \approx 10^{-8}$ at $f_* \approx 1.65$ mHz, yielding SNR ≈ 8.5 for four years of LISA observation at conservative benchmark parameters. The universal f^3 sub-peak slope, independent of all phase-transition parameters and recoverable at $\gtrsim 10\sigma$, constitutes the primary model-independent evidence for a first-order source. A joint LISA–DARWIN detection would constrain the dark confinement scale Λ_{dark}, the latent heat fraction α_{PT}, and the dark matter mass $M_0 = 165.67$ GeV to within factors of 1.5, 1.3, and 2 respectively, establishing a complete multi-messenger characterisation of the $\mathrm{SU}(3)_{\mathrm{dark}}$ dark sector , the GW analysis presented here provides an independent, gravitational-wave-based confirmation of the same dark-sector parameters. the dark Higgs triplet vacuum expectation value $v_\Delta = 17\,\mathrm{GeV}$ and Yukawa coupling $y_\chi = 0.10$ adopted from Ref. [1] carry a theoretical uncertainty of $\pm 10\%$ from the two-loop matching of the effective theory, propagating to a $\pm 5\%$ uncertainty in the tree-level splitting $\Delta M(\chi^+ - \chi^0) = 1.70\,\mathrm{GeV}$. This uncertainty does not affect the GW predictions of the present work, which depend only on the confinement scale Λ_{dark} and the dark gauge coupling g_{dark}.

CODE AND DATA AVAILABILITY

Numerical computations used open-source Python libraries (NumPy, SciPy, SymPy). Code available at:
https://github.com/ahmed19999520-alt/N-body-dark-plasma
For detailed derivations See Supplemental Material at [arXiv -Journal Website]

FUNDING

This article is part of SCOAP^3 open-access agreement.

CONFLICTS OF INTEREST

The author declares no competing financial interests.

[1] A. Ali, *Topological Stability of Dark Matter from $\pi_2(\mathrm{SU}(3)/\mathrm{SO}(3)) = \mathbb{Z}$ with a Dark Higgs Triplet*,[hep-ph] (2026),v2 (arXiv). doi:10.48550/ARXIV.2609.16383

[2] C. Caprini *et al.*, *Science with the Space-Based Interferometer eLISA. II: Gravitational Waves from Cosmological Phase Transitions*, JCAP **04** (2016) 001, DOI:10.1088/1475-7516/2016/04/001, arXiv:1512.06239.

[3] C. Caprini *et al.*, *Detecting Gravitational Waves from Cosmological Phase Transitions with LISA: An Update*, JCAP **03** (2020) 024, DOI:10.1088/1475-7516/2020/03/024, arXiv:1910.13125.

[4] P. Amaro-Seoane *et al.* (LISA Collaboration), *Laser Interferometer Space Antenna*, arXiv:1702.00786 (2017).

[5] J. R. Espinosa, *Energy Budget of Cosmological First-Order Phase Transitions*, JCAP **06** (2010) 028, DOI:10.1088/1475-7516/2010/06/028, arXiv:1004.0993.

[6] M. Hindmarsh, *Numerical Simulations of Acoustically Generated Gravitational Waves at a First Order Phase Transition*, Phys. Rev. D **92** (2015) 123009, DOI:10.1103/PhysRevD.92.123009, arXiv:1504.03291.

[7] M. Hindmarsh and M. Hijazi, *Gravitational Waves from First Order Cosmological Phase Transitions in the Sound Shell Model*, JCAP **12** (2019) 062, DOI:10.1088/1475-7516/2019/12/062, arXiv:1909.10040.

[8] P. Schwaller, *Gravitational Waves from a Dark Phase Transition*, Phys. Rev. Lett. **115** (2015) 181101, DOI:10.1103/PhysRevLett.115.181101, arXiv:1504.07263.

[9] D. Croon, V. Gonçalves, and G. White, *Gravitational Waves from Dark Sector with Confinement*, JCAP

02 (2022) 038, DOI:10.1088/1475-7516/2022/02/038, arXiv:2111.02586.

[10] M. Breitbach, J. Kopp, E. Madge, T. Opferkuch, and P. Schwaller, *Dark, Cold, and Noisy: Constraining Secluded Hidden Sectors with Gravitational Waves*, JCAP **07** (2019) 007, DOI:10.1088/1475-7516/2019/07/007, arXiv:1811.11913.

[11] M. Fairbairn, E. Hardy, and A. Wickens, *Hearing Without Seeing: Gravitational Waves from Hot and Cold Hidden Sectors*, JHEP **07** (2019) 044, DOI:10.1007/JHEP07(2019)044,

[12] J. Halverson, C. Long, A. Maiti, B. Nelson, and G. Salinas, *Gravitational Waves from Dark Yang-Mills Sectors*, JHEP **05** (2021) 154, DOI:10.1007/JHEP05(2021)154, arXiv:2012.04067.

[13] F.-P. Huang and X. Zhang, *Probing the Hidden Gauge Symmetry Breaking through the Phase Transition Gravitational Wave*, Phys. Lett. B **788** (2019) 288-294, DOI:10.1016/j.physletb.2018.11.024, arXiv:1701.04338

[14] R. D. Pisarski and F. Wilczek, *Remarks on the Chiral Phase Transition in Chromodynamics*, Phys. Rev. D **29** (1984) 338, DOI:10.1103/PhysRevD.29.338.

[15] Y. Aoki, G. Endrődi, Z. Fodor, S. D. Katz, and K. K. Szabó, *The Order of the Quantum Chromodynamics Transition Predicted by the Standard Model of Particle Physics*, Nature **443** (2006) 675, DOI:10.1038/nature05120, arXiv:hep-lat/0609068.

[16] P. Arnold and L. G. Yaffe, *Non-Perturbative Dynamics of Hot Non-Abelian Gauge Theories*, Phys. Rev. D **55** (1997) 7760, DOI:10.1103/PhysRevD.55.7760, arXiv:hep-ph/9612305.

[17] A. D. Linde, *Decay of the False Vacuum at Finite Temperature*, Nucl. Phys. B **216** (1983) 421, DOI:10.1016/0550-3213(83)90293-6.

[18] G. Policastro, D. T. Son, and A. O. Starinets, *The Shear Viscosity of Strongly Coupled $\mathcal{N} = 4$ SYM Plasma*, Phys. Rev. Lett. **87** (2001) 081601, DOI:10.1103/PhysRevLett.87.081601, arXiv:hep-th/0104066.

[19] D. Bödeker and G. D. Moore, *Can Electroweak Bubble Walls Run Away?*, JCAP **05** (2009) 009, DOI:10.1088/1475-7516/2009/05/009, arXiv:0903.4099.

[20] A. Kosowsky and M. S. Turner, *Gravitational Radiation from Colliding Vacuum Bubbles: Envelope Approximation*, Phys. Rev. D **47** (1993) 4372, DOI:10.1103/PhysRevD.47.4372, arXiv:astro-ph/9212004.

[21] M. Kamionkowski, A. Kosowsky, and M. S. Turner, *Gravitational Radiation from First Order Phase Transitions*, Phys. Rev. D **49** (1994) 2837, DOI:10.1103/PhysRevD.49.2837, arXiv:astro-ph/9310044.

[22] C. Caprini and R. Durrer, *Gravitational Waves from Stochastic Relativistic Sources: Primordial Turbulence and Magnetic Fields*, Phys. Rev. D **74** (2006) 063521, DOI:10.1103/PhysRevD.74.063521, arXiv:astro-ph/0603476.

[23] B. Allen and J. D. Romano, *Detecting a Stochastic Background of Gravitational Radiation*, Phys. Rev. D **59** (1999) 102001, DOI:10.1103/PhysRevD.59.102001, arXiv:gr-qc/9710117.

[24] T. Robson, N. J. Cornish, and C. Liu, *The Construction and Use of LISA Sensitivity Curves*, Class. Quant. Grav. **36** (2019) 105011, DOI:10.1088/1361-6382/ab1101, arXiv:1803.01944.

[25] E. Thrane and J. D. Romano, *Sensitivity Curves for Searches for Gravitational-Wave Backgrounds*, Phys. Rev. D **88** (2013) 124032, DOI:10.1103/PhysRevD.88.124032, arXiv:1310.5300.

[26] C. Cutler and É. E. Flanagan, *Gravitational Waves from Merging Compact Binaries: How Accurately Can One Extract the Binary's Parameters?*, Phys. Rev. D **49** (1994) 2658, DOI:10.1103/PhysRevD.49.2658, arXiv:gr-qc/9402014.

[27] E. S. Phinney, *A Practical Theorem on Gravitational Wave Backgrounds*, arXiv:astro-ph/0108028 (2001).

[28] G. Agazie *et al.* (NANOGrav Collaboration), *The NANOGrav 15-year Data Set: Evidence for a Gravitational-Wave Background*, ApJL **951** (2023) L8, DOI:10.3847/2041-8213/acdac6, arXiv:2306.16213.

[29] A. Kogut *et al.*, *The Primordial Inflation Explorer (PIXIE)*, JCAP **07** (2011) 025, DOI:10.1088/1475-7516/2011/07/025, arXiv:1105.2044.

[30] J. Chluba *et al.*, *New Horizons in Cosmology with Spectral Distortions of the CMB*, Exp. Astron. **51** (2021) 1515, DOI:10.1007/s10686-021-09729-5, arXiv:1903.04218.

[31] J. Aalbers *et al.* (DARWIN Collaboration), *DARWIN: Towards the Ultimate Dark Matter Detector*, JCAP **11** (2016) 017, DOI:10.1088/1475-7516/2016/11/017, arXiv:1606.07001.

[32] E. Aprile *et al.* (XENON Collaboration), *First Dark Matter Search with XENONnT*, Phys. Rev. Lett. **131** (2023) 041003, DOI:10.1103/PhysRevLett.131.041003, arXiv:2303.14729.

[33] J. Aalbers *et al.* (LZ Collaboration), *First Dark Matter Search Results from the LUX-ZEPLIN Experiment*, Phys. Rev. Lett. **131** (2023) 041002, DOI:10.1103/PhysRevLett.131.041002, arXiv:2207.03764.

[34] N. Aghanim *et al.* (Planck Collaboration), *Planck 2018 Results VI: Cosmological Parameters*, A&A **641** (2020) A6, DOI:10.1051/0004-6361/201833910, arXiv:1807.06209.

[35] D. J. Gross and F. Wilczek, *Ultraviolet Behavior of Non-Abelian Gauge Theories*, Phys. Rev. Lett. **30** (1973) 1343, DOI:10.1103/PhysRevLett.30.1343.

[36] H. D. Politzer, *Reliable Perturbative Results for Strong Interactions?*, Phys. Rev. Lett. **30** (1973) 1346, DOI:10.1103/PhysRevLett.30.1346.

[37] K. Kajantie, M. Laine, K. Rummukainen, and M. Shaposhnikov, *Generic Rules for High Temperature Dimensional Reduction*, Nucl. Phys. B **458** (1996) 90, DOI:10.1016/0550-3213(95)00549-8, arXiv:hep-ph/9508379.

[38] M. Dine, R. G. Leigh, P. Huet, A. Linde, and D. Linde, *Towards the Theory of the Electroweak Phase Transition*, Phys. Rev. D **46** (1992) 550, DOI:10.1103/PhysRevD.46.550, arXiv:hep-ph/9203203.

[39] S. Tulin and H.-B. Yu, *Dark Matter Self-Interactions and Small Scale Structure*, Phys. Rept. **730** (2018) 1, DOI:10.1016/j.physrep.2017.11.004, arXiv:1705.02358.

[40] G. Jungman, M. Kamionkowski, and K. Griest, *Supersymmetric Dark Matter*, Phys. Rept. **267** (1996) 195, DOI:10.1016/0370-1573(95)00058-5, arXiv:hep-ph/9506380.